ENTROPY WAVE GENERATOR FOR INDIRECT COMBUSTION NOISE EXPERIMENTS IN A HIGH-PRESSURE TURBINE

P. Gaetani, G. Persico, A. Spinelli

Dip. Energia, Politecnico di Milano, via Lambruschini, 4 – 20158 Milano, Italy;
paolo.gaetani@polimi.it

C. Sandu

SMCPFA, 6A Ripiceni str., Bl.5, Ap.40, Sector2, Bucharest, Romania

F. Niculescu

COMOTI, 220D Iuliu Maniu bvd., Sector 6, Bucharest, Romania

ABSTRACT

The reduction of core-noise represents a crucial objective for the deployment of low noise propulsion systems. In this context the European Project RECORD - REsearch on COre noise ReDuction - aims at quantifying the impact of the turbine on direct and indirect combustion noise by means of a set of dedicated experiments carried out on an engine representative high pressure turbine, installed in the high-speed test rig of Politecnico di Milano (Italy). The aero-acoustic interaction of pressure, vorticity, and entropy waves with the turbine will be studied.

This paper presents a novel Entropy Wave Generator (EWG) to simulate the entropy perturbations originated by gas turbine burners. The device, designed and manufactured by SMCPFA (Romania), is based on the alternated injection of hot/cold air upstream of the turbine, by using a two-way rotary valve. The entropy waves generated by the EWG were experimentally characterized in a dedicated test section at Politecnico di Milano. Tests were performed using different insulation systems, and investigating the propagation of entropy waves in both free-jet and immersed-jet configurations. Tests were performed by means of a fast thermocouple (frequency response ~300 Hz) and a pneumatic total pressure probe (frequency response ~400 Hz), specifically developed for the project. Results indicate that for an optimal feeding pressure the EWG generates circular-shaped spots of hot air characterized by a sinusoidal temperature fluctuation and weak pressure oscillations; the amplitude of the temperature oscillation reduces as the frequency increases, however resulting higher than 10 K at the engine-representative frequency of 100 Hz. This value matches the technical requirements of the EWG, making it suitable for entropy noise studies in the turbine test rig.

NOMENCLATURE

c, ρ	specific heat and density of the thermocouple junction
D	diameter of the thermocouple wire/junction
h	convective heat transfer coefficient
x, y, z	horizontal, vertical and axial coordinates (for immersed-jet tests)
P_{EWG}, n_{EWG}	EWG feeding pressure, EWG rotary valve angular speed
P, T	Total Pressure, Total Temperature of the flow
$\Delta P/\Delta P_{shock}$; $\Delta T/\Delta T_{shock}$	Gauge total pressure, temperature normalized to that across the shock
ΔT	Amplitude of the total temperature fluctuation of the entropy wave
Φ	Phase on the entropy wave pulsation period

INTRODUCTION

In view of reducing the environmental impact of aero-engines, the control of the aerodynamic noise represents a key objective, with several open issues still demanding significant research efforts. The concept of aerodynamic noise was originally introduced by Lighthill (1952, 1954), who showed that, in non-quiescent fluids, a number of aerodynamic phenomena may induce small pressure oscillations, namely acoustic effects. The so-called Lighthill analogy reveals that Reynolds stresses, viscous forces and non-isentropic flows act as sources of sound (Rienstra and Hirschberg, 2015); therefore noise is generated by turbulence, by time-dependent coherent flow structures (vortex sound), and by unsteady entropy waves. All of these mechanisms act in aero-engines, due to the complex flow configuration and the unsteady heat release commonly found in these devices.

In the last decades comprehensive studies and improved technical solutions allowed to significantly reduce the fan and jet noise in aero-engines; this, combined with the use of highly-loaded turbines and lean combustors in present day engines (Cumpsty, 1979), has made more significant the so-called engine 'core-noise' (Bake, 2007), namely the contribution provided by the combustor and by its acoustic matching with the High Pressure (HP) turbine.

Two very different mechanisms contribute to the engine core-noise: (I) the unsteady heat release in the burners produces sound by itself, commonly referred to as 'direct' combustion noise; the acoustic waves generated by the burner interact with the turbine flow, so the total noise radiated by the engine strictly depends on the acoustic matching between the combustor and the turbine; (II) the unstable character of the flame also leads to time-dependent vorticity fluctuations and entropy waves (Dowling, 1996) that, once accelerated by the turbine nozzle, act as sources of sound, producing further noise (Marble and Candel, 1977, and Cumpsty and Marble, 1977). The latter mechanism, resulting from the aero-acoustic coupling between the combustor and the turbine, is commonly referred to as 'indirect' combustion noise. Detailed theoretical studies suggest that the indirect entropy noise provides a relevant contribution to the core-noise of real-engines (Cumpsty, 1979), even exceeding the contribution of the direct combustion noise (Leyko at al., 2009).

To achieve core-noise attenuation a detailed knowledge of all the basic generation mechanisms is crucial; standard experiments on combustors are de-facto of limited use, as a proper distinction between direct and indirect combustion noise is very difficult (Muthukrishnan et al, 1978). To overcome that limitation, specific experiments were designed so to study the indirect noise only, by eliminating any direct source noise; in these experiments the combustors are replaced by devices designed to produce unsteady entropy waves, that are subsequently accelerated in nozzles. The first experiment on indirect combustion noise was performed by Bohn (1976) and Zukoski and Auerbach (1976), who used electrical heaters to generate entropy waves of limited amplitude ($\Delta T \cong$ 1 K). More recently Bake et al. (2009) designed an Entropy Wave Generator (EWG) test rig to perform canonical experiments on entropy noise. In that test rig the entropy waves are obtained by producing, via electrical heaters, controlled 'slugs' of hot fluid ($\Delta T \cong 10$ K); experiments confirmed that the acceleration of the entropy waves produces noise. Subsequent theoretical models were proposed to explain this experimental finding, shedding some light on the physics of entropy noise generation in accelerating flows (Bake et al., 2009, Leyko et al., 2011, Howe, 2010).

These recent results, even though obtained in nozzles and with a simplified entropy wave configuration, indicate that indirect combustion noise may be relevant in gas turbine engines, and make it worth of further research in more realistic environments. This represents one of the motivations of European Project RECORD, in whose frame indirect combustion noise is studied in a test-rig where a realistic HP turbine stage is installed. To guarantee the engineering relevance of the experiment, a novel EWG has been specifically developed to simulate the actual character of the time-dependent entropy field produced by unstable flames in the burners.

In the present paper the experimental set-up, the design, and the characterization of the EWG is discussed. At first the test rig layout is reviewed in detail and the EWG operational principle is described; then the character of the entropy waves generated by the device in both still air and confined flow configuration are discussed in detail.
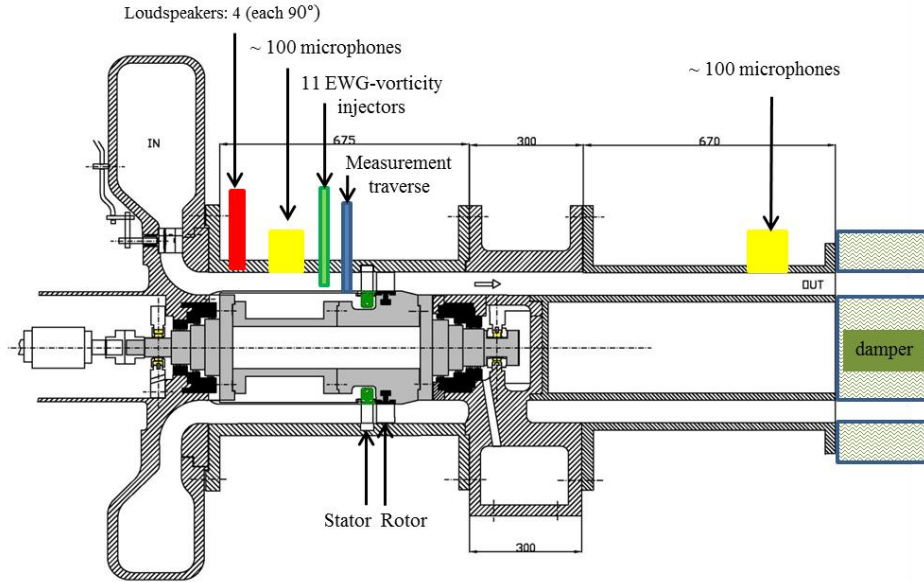
Figure 1: Schematic view of the test rig for indirect combustion noise experiment in a HP turbine

INDIRECT COMBUSTION NOISE EXPERIMENT

The experiments on indirect combustion noise in a HP turbine will be performed in the high-speed closed-loop test rig operating in the Laboratorio di Fluidodinamica delle Macchine (LFM) of Politecnico di Milano (Italy). The test rig is composed by the compressor station, constituted by a high-speed centrifugal compressor and a cooler, that provides flow rate to the turbine section, where a HP gas turbine stage is mounted. The two machines are connected to two reversible DC engines that allow a continuous and independent regulation of the rotational speed, in such a way that the angular speed and the expansion ratio of the turbine can be assigned independently. The HP turbine model is representative of a present-day highly loaded and low aspect ratio stage operating in subsonic/transonic conditions (maximum Mach number ~0.9 at the stator exit). Full details on the test rig and the HP turbine stage can be found in Gaetani et al. (2007a); the unsteady flow and blade row interaction of this turbine stage, operated in subsonic conditions, were extensively studied by the authors (Gaetani et al., 2007b, Persico et al., 2009, Gaetani et al., 2010, Persico et al., 2012).

A meridional cut of the turbine section is depicted in Figure 1. The turbine stage is fed by a centripetal guide vane composed by 30 high-lift profiles, specifically designed to deflect the flow from highly tangential direction at the exit of the volute (~70° from radial direction) to nearly meridional direction at the inlet of the axial section; to guarantee flow uniformity at the turbine inlet a straightener (honeycomb) is mounted downstream of the centripetal section. Downstream of the honeycomb a relatively long (400 mm) straight annular section is left upstream of the stator leading edge; in this duct two devices are introduced to simulate the direct and indirect acoustic effect of the combustor: a loudspeaker, that generates a controlled acoustic field upstream of the turbine; a row of EWG injectors, used to simulate entropy (and possibly vorticity) perturbations and/or steady hot streaks coming from the burners. In-between the two devices, a system of ~100 microphones is mounted to synthesize the incoming acoustic field.

To guarantee a simple spatial periodicity, one injector out of two stator blades is installed (11 injectors in total over 22 stator blades). Downstream of the stage, a long straight section is introduced, where a system of further ~100 microphones is assembled to measure the direct and the indirect noise generated or transmitted across the turbine.

Time-averaged and time-resolved aerodynamic and temperature measurements will be performed, to fully characterize the flow and thermal fields at the inlet and exit of the turbine, as well as in-between the blade rows. Fast response ThermoCouples (FTC, frequency response ~300 Hz), Fast Response Aerodynamic Pressure Probes (FRAPP, frequency response ~80 kHz), and pneumatic five-hole probes will be applied.

EWG SYSTEM LAYOUT

The Entropy Wave Generator (EWG) here presented simulates the high/low entropy spots released by burners by injecting alternatively hot and cold air at prescribed frequency in the turbine duct. The equipment was conceived, designed and manufactured by SMCPFA (Romania). The technical requirements for the EWG in order to properly represent the burner can be synthesized as follows: temperature fluctuation ΔT equal to 4%÷40% of the mean flow temperature (which is ~330 K in the present cold-flow test rig); frequency content of the disturbances of 100 Hz; maximum radial traversing of 50 mm, to cover the whole channel span. The injection of entropy waves will be at 70% span, namely 15 mm below the casing: this allows to minimize the blockage effect of the injectors and to avoid the interaction between the entropy waves and the stator secondary flows.

Basic operating principle

The conceptual scheme of EWG operating principle is presented in Figure 2. Cold compressed air coming from LFM line is split into 2 streams. One stream is kept cold and the other is heated by an electrical heater. The alternation between hot and cold air streams is generated by a rotary valve actuated by a high precision electrical servo-motor. The EWG rotary valve features two cross holes, that alternatively open the cold or the hot stream in such a way that, when cold air passes, the air to be heated is blocked and vice-versa.

The nominal frequency of hot-cold pulses is set to 100 Hz, and it is achieved by running the rotary valve at 3000 rpm (or 50 Hz, since the EWG generates two perturbations for each rotation). Downstream of the rotor and of the heater, the hot and cold air pulses are split into 11 hot and 11 cold air streams by two conical distribution boxes (hot box and cold box), transported through 22 tubes (11 cold and 11 hot); the hot and cold tubes are finally connected just upstream of 11 metal injectors, which are installed in the turbine test rig duct. Figure 2 also provides the expected trends of flow rate and temperature detected downstream of the injector. Despite the rapid alternation between the two streams, the temperature signal (and hence the entropy perturbation, as the pressure is roughly constant) is expected to be significantly smoothed as the mixing process and the heat transfer take place between hot and cold parts in the injector. A sinusoidal entropy signal is then expected to be injected in the flow incoming in the turbine. The amplitude of the oscillations is strictly depending on the flow rate (and hence on the EWG feeding pressure), on the thermal power exchanged through the heater and on the insulation of the injectors and of the tubes. This latter, in particular, represents a crucial feature that is discussed in detail in the following Sections.
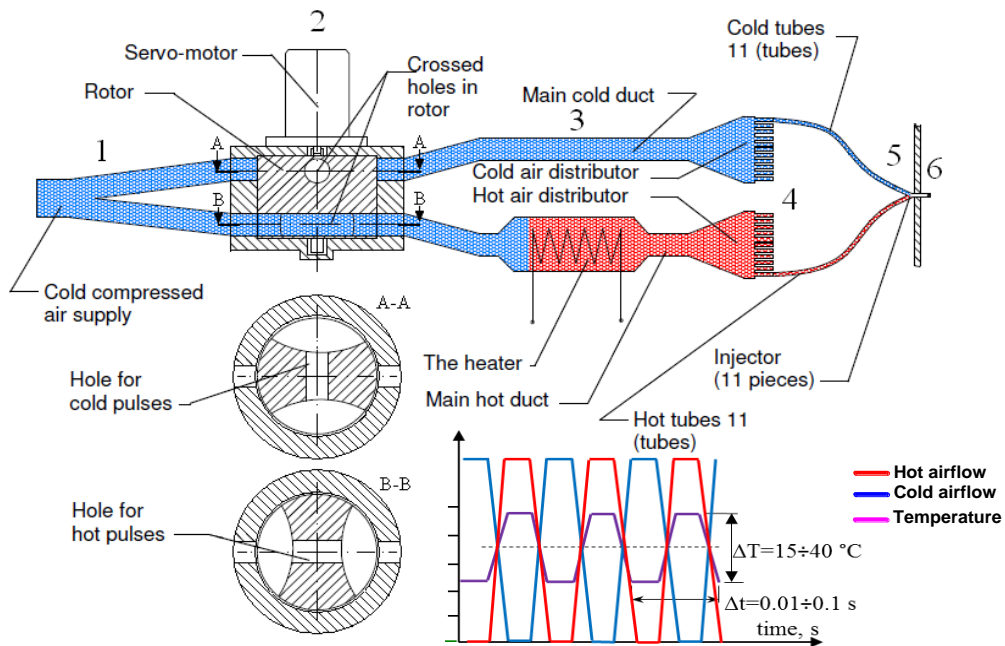

Figure 2: Scheme of the EWG operating principle and expected temperature fluctuation

Design

The EWG assembly contains 77 individual P/Ns. The servo-motor, controlled by the AC Servo-Drive, guarantees an extremely precise regulation of the pulse frequency (within 0.01% Hz). The EWG operation is controlled by means of two consoles, namely the 'Air-control console' and the 'Electrical-control console'. On the Air-control console are placed ball-valves, manometers and flow-meters for measuring air parameters in the two air circuits. On the Electrical-control console are placed the DC power supply (transforming 220 V AC in DC low voltage), the temperature regulator, the temperature indicator, and the static relay.

INSTRUMENTATION

Miniaturized and fast-response instrumentation is required to characterize the time-dependent pressure and temperature fields provided by the EWG injectors. A piezo-resistive pressure sensor (Kulite XT 190, full scale 1.7 bar, uncertainty ± 80 Pa) was also introduced in one of cold tubes of the EWG, to monitor the feeding pressure and to provide a trigger signal for ensemble averaging. In the frame of this research a miniaturized Pneumatic Total Pressure probe (PTP) and a Fast micro-ThermoCouple probe (FTC) were designed, manufactured and dynamically calibrated in the low pressure shock tube available at Politecnico di Milano (Persico et al., 2005).

PTP design and dynamic performance

The total pressure probe was designed as an L-shaped device, whose dimensions were minimized considering the constraints imposed by the test section; the probe is characterized by a frontal section diameter of 1.5 mm, a straddle of 10 mm and a 200 mm stem, that connects the pressure tap (diameter 1 mm) to a piezo-resistive pressure sensor (Kulite XT 190 V74-29, full scale 0.35 bar, uncertainty ± 80 Pa). The resulting line-cavity system resonance frequency was estimated equal to ~300 Hz by applying the thermal-viscous acoustic model proposed by Antonini et al. (2008). Calibration tests in the shock tube showed a good dynamic linearity of the device (typical of a second order system) with resonance frequency at ~250 Hz. The frequency response of the probe, after digital compensation with the experimental transfer function, can be extended to 400 Hz, largely matching the requirements of the present application.

FTC design and development

The development of fast-response temperature instrumentation represents a challenging task that demands specific development. Considering the frequency range of interest for the entropy waves and the relatively harsh environment of the facility, a thermocouple probe was selected as the most suitable measurement device for the present application. However the development of sufficiently fast thermo-couple probes requires a dramatic miniaturization and advanced manufacturing tools.

The probe is based on Platinum / Platinum-Rhodium wires (S-type thermocouple, uncertainty ± 0.2 K) to avoid oxidizing and to ease the welding process of the wires. The core of the design was the selection of the diameter of the wire, in connection to the dynamic response of the instrument. The heat transfer process of a miniaturized thermocouple junction immersed into a flow stream can be treated with a lumped parameter approach; the dynamics of the junction, here assumed of cylindrical shape, can be modelled as a first order linear system, whose time constant results:

$$\tau \triangleq \frac{\rho c D}{4\,h}. \tag{1}$$

The dynamic response of the thermocouple was theoretically estimated by resorting to the Churchill and Bernstein correlation (Churchill and Bernstein, 1977); calculations indicated that to exceed a frequency response of 100 Hz the maximum diameter acceptable for the wires is 25 μm.

Two micro FTC probes, characterized by wire diameters equal to 25 μm and 12.5 μm, were manufactured and tested in the shock tube, in which the sweeping of the shock front produces a total temperature step signal. Experiments showed a very good dynamic linearity of the FTC
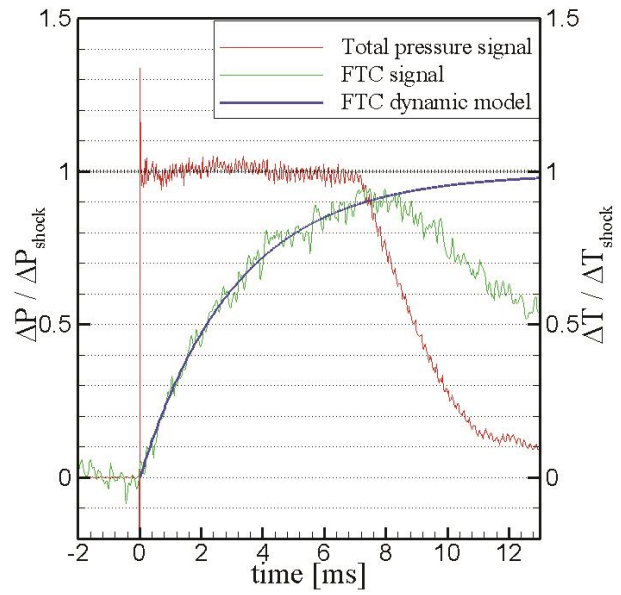
Figure 3: FTC junction (25 μm) (left) and experimental step response in the shock tube (right).

probes, and a good quantitative agreement with the prediction of the correlation (~10% error in the estimate of the time constant). The 12.5 μm FTC exhibited an excellent promptness (~1.2 ms of time constant, namely ~400 Hz of frequency response after digital compensation) but resulted too fragile for routine application in the facility (which should run continuously for 5-10 hours). Conversely the 25 μm FTC, whose step response is reported in Figure 3 alongside a picture of its junction, exhibited an acceptable promptness (~2.5 ms of time constant, namely ~200 Hz as frequency response after digital compensation) and an excellent rigidity and reliability both in shock tube and wind tunnel tests. This latter configuration was hence selected as temperature measurement system for the whole research, also considering that even faster dynamic response (~300 Hz) will be achieved in the test rig, thanks to the higher pressure level of the flow at the turbine inlet with respect to the post-shock value.

PROPAGATION OF ENTROPY WAVES IN STILL AIR

Prior to characterize the pressure and temperature fields generated by the EWG injecting into a flow stream, a preliminary experimental analysis was performed with the injector discharging in still air. These measurements were instrumental to quantify the amplitude and the frequency content of the temperature fluctuations achievable with the device, and allowed a relatively easy evaluation of the effectiveness of several insulation systems. For these tests the spatial reconstruction of the
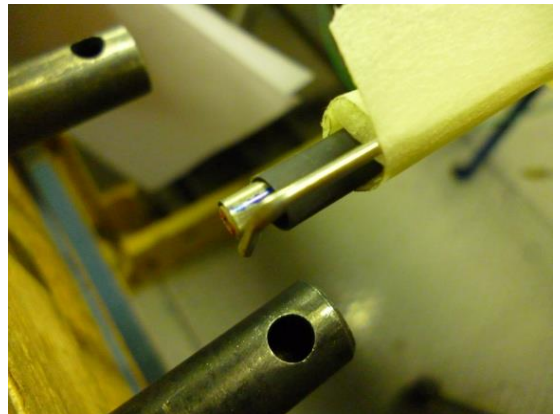

Figure 4: Free-jet tests. Left: tubes and injectors set-up (insulation: ceramic fiber + 5 mm elastomeric sheath). Right: probe position (not aligned with the jet to improve visibility)

high/low entropy waves was not of interest; hence free-jet tests were performed in a fixed position in space, with probes placed in front of and very close to the injection holes (1 mm downstream). Temperature measurements with standard thermo-couples were also performed downstream of the heating section and at the end of the hot tubes, to monitor the temperature drops across both the hot tubes and the injectors.

Pressure and temperature signals

Figure 5 shows two examples of total pressure and total temperature signals measured in free-jet conditions, achieved with EWG feeding pressure of 1.4 bar; both the quantities exhibit a dominant periodicity, the temperature being characterized by an almost sinusoidal trend; the pulsation frequency, as expected, can be correlated as twice the rotation frequency of the EWG rotary valve.

The total pressure signal exhibits a higher dynamic content than that of the temperature; this can be explained by considering the way in which the alternated hot/cold streams in the tubes merge themselves just upstream of the injector; even though all the tubes have the same length, small delays may exist between the two streams, also because of the different enthalpy levels of hot and cold streams. These delays induce small phase displacements that eventually result in a highly fluctuating pressure signal. These effects are smoothed in the temperature signal due to the mixing between the streams that occurs as the hot and cold spots travel in the injector.

From the quantitative point of view, the total pressure oscillations are within ~4 mbars, which means far less than 1% of the average flow pressure level (~1 bar in the free-jet tests); hence, the pressure contribution to entropy perturbation is minimal; the subsequent velocity perturbation, and its potential contribution to the hydrodynamic indirect noise, is not relevant in free-jet tests and will be addressed when discussing immersed jet tests. The total temperature oscillation is, instead, very significant in free-jet tests. Figure 5 shows that, at 300 rpm, or 10 Hz of fundamental frequency, the temperature oscillation amounts to ~40 K, more than 10% of the mean temperature level in the jet (equal to ~360 K). Tests performed throughout the measurement campaign showed a very good repeatability of the signals, in terms of both amplitude and frequency. However, as shown in Figure 6, the amplitude changes with the EWG angular speed; in particular, as the fundamental frequency is enhanced, the amplitude of temperature fluctuation reduces, up to 15 K in case of 3000 rpm, or 100 Hz, which means 4% of the mean temperature level.

Insulation system improvement

The temperature fluctuations measured in free-jet tests match the targets set for the EWG; however the real amplitude of fluctuations in immersed jet conditions was expected to significantly reduce, due to the mixing between the EWG jet and the surrounding cold flow. For this reason, prior to focus on immersed-jet tests a specific study was performed to improve the insulation
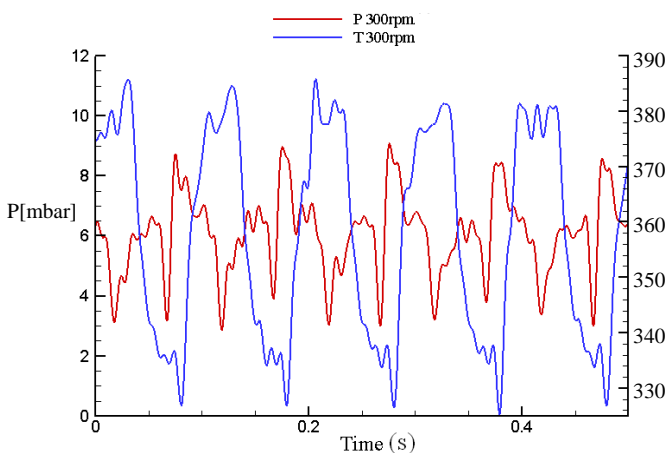

Figure 5: Raw pressure and temperature signals acquired in free-jet tests for 300 rpm (i.e., 10 Hz fundamental frequency)
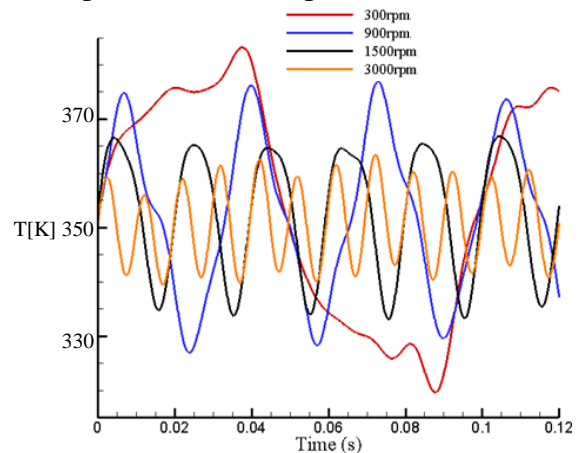
Figure 6: Temperature signals (after dynamic compensation) for different angular speed of the EWG rotary valve

system of the EWG. The original configuration, in which the measurements shown in Figures 5 and 6 were taken, consisted in hot tubes made of Polytetrafluoroethylene (PTFE, melting point 327°C) insulated by positioning all of them between two 100 mm thick plates of mineral fibers. However, the constraint of the test rig require that the different tubes are mounted independently and must be insulated individually.

An analysis of the temperature drops in the hot parts of the EWG clearly showed that the most critical issue of the device is the insulation of the eleven hot tubes that connect the heating section of the EWG with the eleven injectors (~200 K of drop in the original configuration). To insulate the tubes ceramic fiber was used, which reduced the temperature drop by almost a factor 2, but also required to reduce the maximum heater temperature due to limitations on the hot tubes material. As reported in Table 1, the maximum temperature at the end of the hot tubes (so, just upstream of the injector) reduced to 360 K in this second set-up.

To improve the insulation of the tubes, an additional element was added, made of elastomeric material and characterized by a thickness of 5 mm; this system allowed to further reduce the temperature drop to 40 K. This third configuration was further improved by substituting the 5 mm thick tubes with 19 mm thick tubes made of a more resistant material, so to improve the heater temperature. In this way the maximum temperature at the inlet of the injectors was raised to 420 K.

This was the insulating condition used for the immersed jet tests, even though further temperature increase is possible by working with proper materials.

Configuration	Heater temperature [K]	Maximum injector temperature [K]
1	590	390
2	490	360
3	410	370
4	460	420

Table 1. Temperature of the different insulating configurations.

PROPAGATION OF ENTROPY WAVES WITHIN UNIFORM FLOW STREAM

In order to investigate the real character of the entropy waves generated in the turbine test rig proper tests with injectors immersed into a flow stream were performed. To simulate the test-rig configuration, a uniform flow stream with Mach number in the range 0.1÷0.15 and total temperature of 320÷330 K is required. The stream was generated by connecting a calibrated nozzle to the blow-down wind tunnel operating at LFM. Downstream of the nozzle, whose square exit section is of 0.08 m side, a straight prolongation was added where one of the injectors was inserted, as shown in the left frame of Figure 7. The FTC and PTP probes were traversed just downstream of the exit section of the tunnel (see the central frame of Figure 7) where, as resulted from the nozzle calibration, the open jet discharged by the tunnel retains the feature of a wall-bounded flow, both for the mean flow and turbulence properties (such a feature lasts for an axial extension of ~2 jet width, or ~0.15 m). In the following the unsteady total pressure field is first discussed, then the total temperature perturbations are analyzed.

Unsteady total pressure field

The flow discharged by the tunnel was first analyzed by considering the total pressure distribution measured downstream with the PTP. Given the design and layout of the wind tunnel, uniform static pressure is expected in this region, so the total pressure gradients here measured can be mainly interpreted as velocity gradients. The right frame of Figure 7 provides the total pressure distribution measured in a position corresponding to the turbine stator inlet, and indicates that the total pressure field is almost uniform in the injection area. Significant gradients are observed towards the left wall of the tunnel, where the wake of the cylindrical injector interacts with the wall boundary layer. The flow uniformity observed in the injection region might be due to the
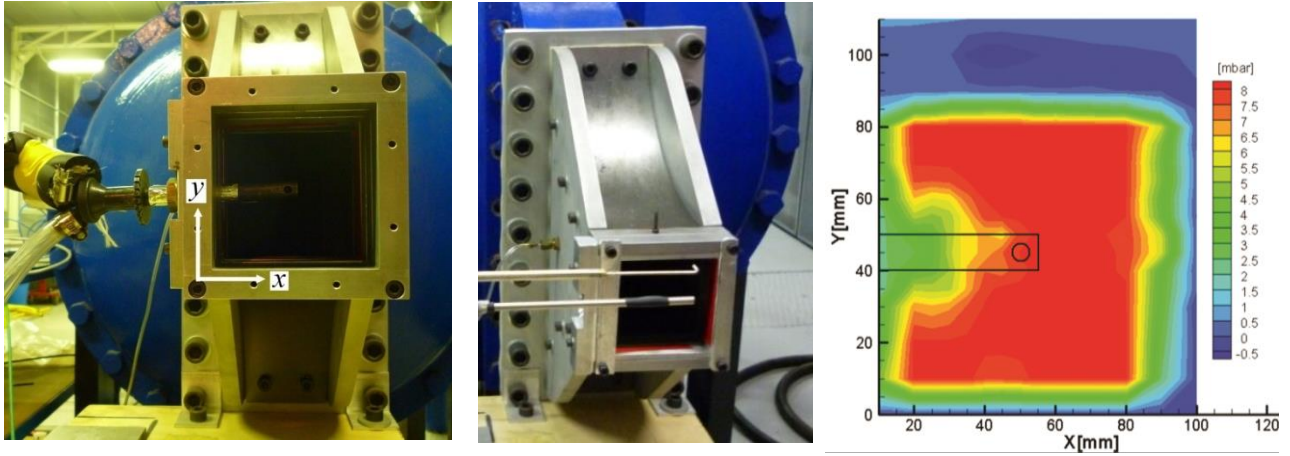
Figure 7: Immersed-jet tests. Left: wind tunnel discharge section and EWG injector position. Center: probe position and traversing. Right: total pressure distribution 55 mm away from the injector (corresponding to the stator LE position in the test rig) with injector sketch overlaid.

'stabilizing' effect of the injection itself, which provides momentum into the dead water zone in the trailing region of the cylinder; however, this also indicates that a significant mixing takes place between the jet produced by EWG and the surrounding flow; this inevitably smears the temperature gradients leading to a deamplification as the waves propagate into the flow.

The unsteady evolution of the total pressure field was also analyzed in detail. Significant dynamic content was observed in the zone downstream of the injector, in the frequency range 700÷900 Hz (even without dynamic compensation of the signal); this is consistent with the injector vortex shedding frequency, which can be estimated (assuming Strouhal number 0.21) as 720 Hz in the present operating condition. However this frequency range is by far higher than the one of interest for the indirect noise experiments under consideration. Small total pressure oscillations at the EWG fundamental frequency were also observed in a position corresponding to the injection hole; the amplitude of these oscillations was observed to decay from 1 to 0.3 mbar passing by 20 to 55 mm away from the injector hole. In this latter position (corresponding to the distance between the EWG injector and the turbine inlet in the test-rig application), this means a ~3% velocity perturbation and is expected to have a negligible impact on indirect noise generated in the turbine.

Unsteady total temperature field

The character of the temperature perturbations generated by the EWG in a uniform flow stream represents the most interesting feature of the present work, and it is crucial for the ongoing indirect noise experiment. Beside the amplitude and frequency of the oscillations, also the shape and spatial extension of the waves propagating in the flow are of interest. To provide a proper description of the entropy waves the FTC was traversed in the region around the injector with 1 mm spatial resolution. For these tests the effects of the EWG feeding pressure, of the EWG rotor angular speed, and of the distance between the probes and the injection holes were addressed. The 'performance' of different EWG injectors were also compared, to verify the coherency between the different branches of the device. Differences within 1 K in amplitude of temperature fluctuations were found.

Figure 8 provides the mean and fluctuating temperature fields measured 55 mm downstream of the injector hole (test-rig representative), for the EWG rotor running at 3000 rpm and the feeding pressure set to 1.4 bar. The mean temperature distribution (left frame) clearly marks the presence of a region of hot fluid of elliptical shape, roughly centered at the injector hole (note that the temperature maps are shifted vertically by ~20 mm with respect to the pressure map due to the different vertical positions of the pressure and temperature probes, see the central frame of Fig. 7). In order to provide a comprehensive image of the unsteady temperature fluctuation over the measurement section, the amplitude of the oscillation was determined point by point on the measurement grid. Due to the sinusoidal character of the temperature signals, this corresponds to
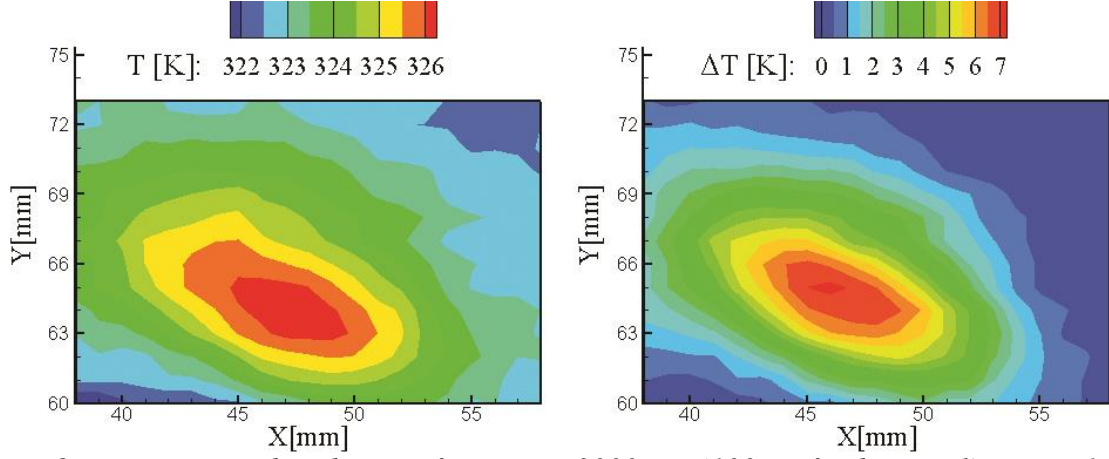
Figure 8: Temperature distributions for n_{EWG} = 3000rpm (100 Hz fundamental), P_{EWG}=1.4 bar, z = 55mm. Left: mean profile. Right: amplitude of fluctuation at 100 Hz.

the amplitude of the harmonic at the EWG fundamental frequency. The unsteady distribution shows a very good correspondence with the mean one, with higher gradients with respect to the background flow. The correspondence between mean and fluctuating distributions can be explained by considering that, in these tests, the cold streams of the EWG were at almost the same temperature of the background flow; thus only the hot streams constitute the entropy waves, as it actually occurs in real engines.

The amplitude of the temperature oscillation exhibits a significant drop with respect to free-jet tests, resulting ~7 K despite the insulation system used for immersed-jet tests is by far more effective than that used for the free-jet tests. This is mostly due to the mixing experienced by the EWG jet and the surrounding flow, as it can be inferred from the results of measurements performed much closer (20 mm downstream) to the injectors. As it is visible from the distributions provided in Figure 9, in this position the temperature oscillations amount to tens of K as found in free-jet tests, being larger for lower fundamental frequency. It is interesting to note that the shape of the entropy wave also changes significantly as it propagates in the flow, passing from an elliptical structure elongated in vertical direction (so, normal to the injector axis) close to the injector to a mainly horizontal elliptic trace in the farthest downstream plane – even though the injector hole has circular shape.

The mixing of the EWG jet with the surrounding flow mainly depends on the EWG feeding pressure; a low momentum jet immersed in a flow stream undergoes a relevant decay, being smeared as a wake; a too high momentum jet also triggers significant diffusion processes as in an ejector. Therefore an optimal EWG feeding pressure does exist, so to provide comparable momentum level between the jet and the surrounding flow. Figures 8 and 9 suggest that a feeding
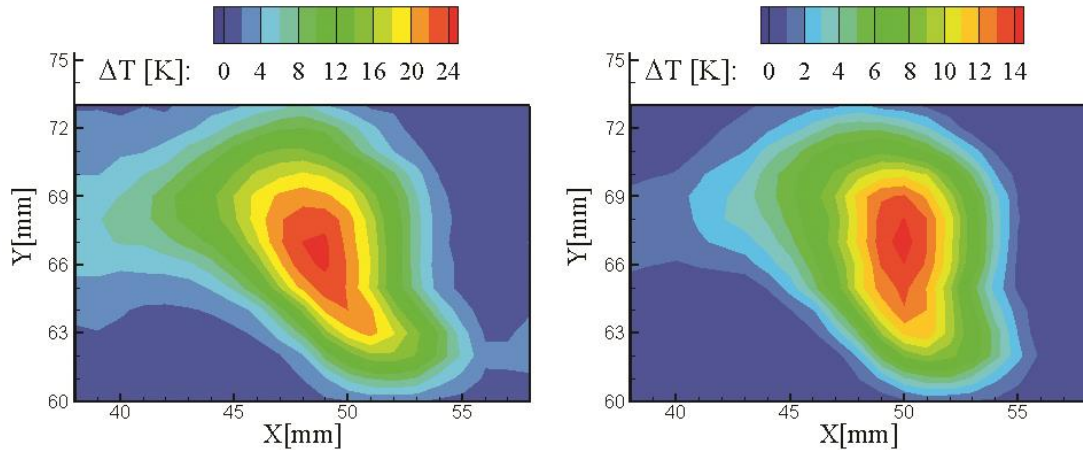

Figure 9: Temperature fluctuations at z = 20 mm, P_{EWG}=1.40 bar for n_{EWG} = 300 rpm, or 10 Hz (left), and for n_{EWG} = 3000 rpm, or 100 Hz (right)
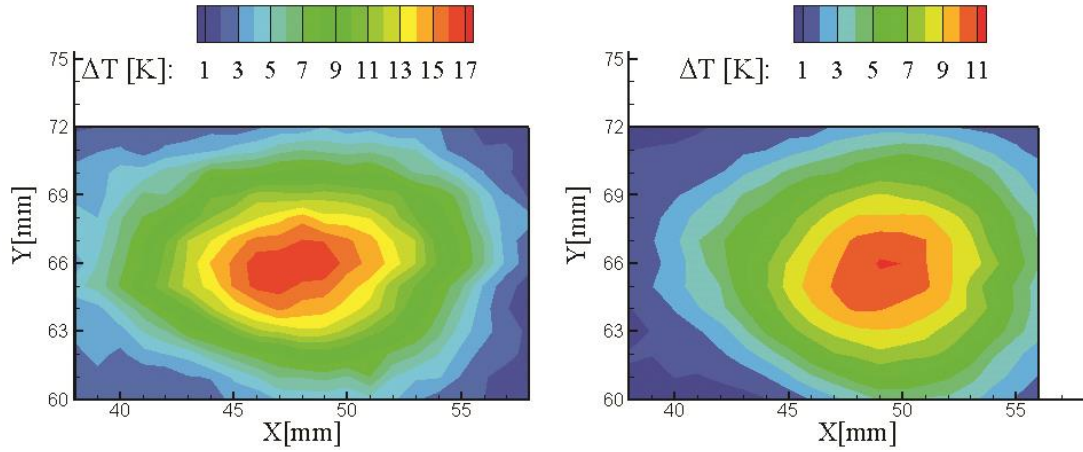
Figure 10: Temperature fluctuations at z = 55 mm, P_{EWG}=1.80 bar for: left, n_{EWG} = 300 rpm, or 10 Hz; right: n_{EWG} = 3000 rpm, or 100 Hz

pressure of 1.4 bar does not provide sufficient momentum to the jet; therefore some tests with larger EWG feeding pressure were performed and eventually an optimal value of 1.8 bar was identified.

Figure 10 reports the total temperature fluctuations measured with higher feeding pressure in the test-rig representative distance. Qualitative and quantitative differences appear in the entropy wave with respect to the lower feeding pressure configuration. The shape of the entropy wave results much less elongated, the hot core appearing as a circular area of diameter 6-8 mm centered on the injector hole position. Considering that the EWG injector has a circular hole of diameter equal to 5 mm, these measurements suggest that the entropy wave generated in this condition keeps its coherence during the propagation in the flow. As a result of the reduced mixing, the temperature oscillation connected to the entropy wave rises to 17 K at 10 Hz and to 11 K at 100 Hz, i.e. 5.5% and 3.5% of the mean temperature level respectively. These features are in line with the targets of the project, and outperform other EWG devices presently available both in terms of frequency content and amplitude.

To provide a time-dependent representation of the entropy wave generated by the device, an ensemble averaging process was applied to the total temperature signals acquired on the measurement grid. The TTL signal from the EWG rotor not being available, the unsteady pressure signal measured on the cold tube just downstream the rotary valve was used as key-phasor; such a signal was observed to exhibit a very good repeatability and reliability during all the tests. The total temperature signals acquired in different points on the measurement grid were first phase-locked to the key-phasor and then phase-averaged so to retain only the dynamic content at the fundamental frequency (higher harmonics provided negligible contribution), while filtering the small non-periodic components. The resulting periodic signals were eventually collected in a phase-resolved flow field, whose temporal evolution is shown in Figure 11 for 100 Hz as fundamental frequency. The different frames show the character of the entropy waves: as already discussed, and well visible at the beginning of the period (ϕ = 0.0), the cold stream of the EWG is at almost the same temperature of the background flow, so the entropy wave appears as periodic pulsation of hot fluid; the plots of Figure 11 also show that the circular shape of the entropy wave is retained during the whole the period, further confirming the coherence of the entropy wave generated.

CONCLUSIONS

In this paper the design and the experimental assessment of a novel Entropy Wave Generator has been presented. The device was conceived to support engine-representative experiments on indirect entropy noise in a high pressure turbine; to generate periodic entropy perturbations, a systems composed by a two-way rotary valve and an electric heater is assembled so to alternatively release hot and cold air spots. In this way controlled jets with periodic temperature profile are injected upstream of the turbine by eleven injectors installed in the test-rig.
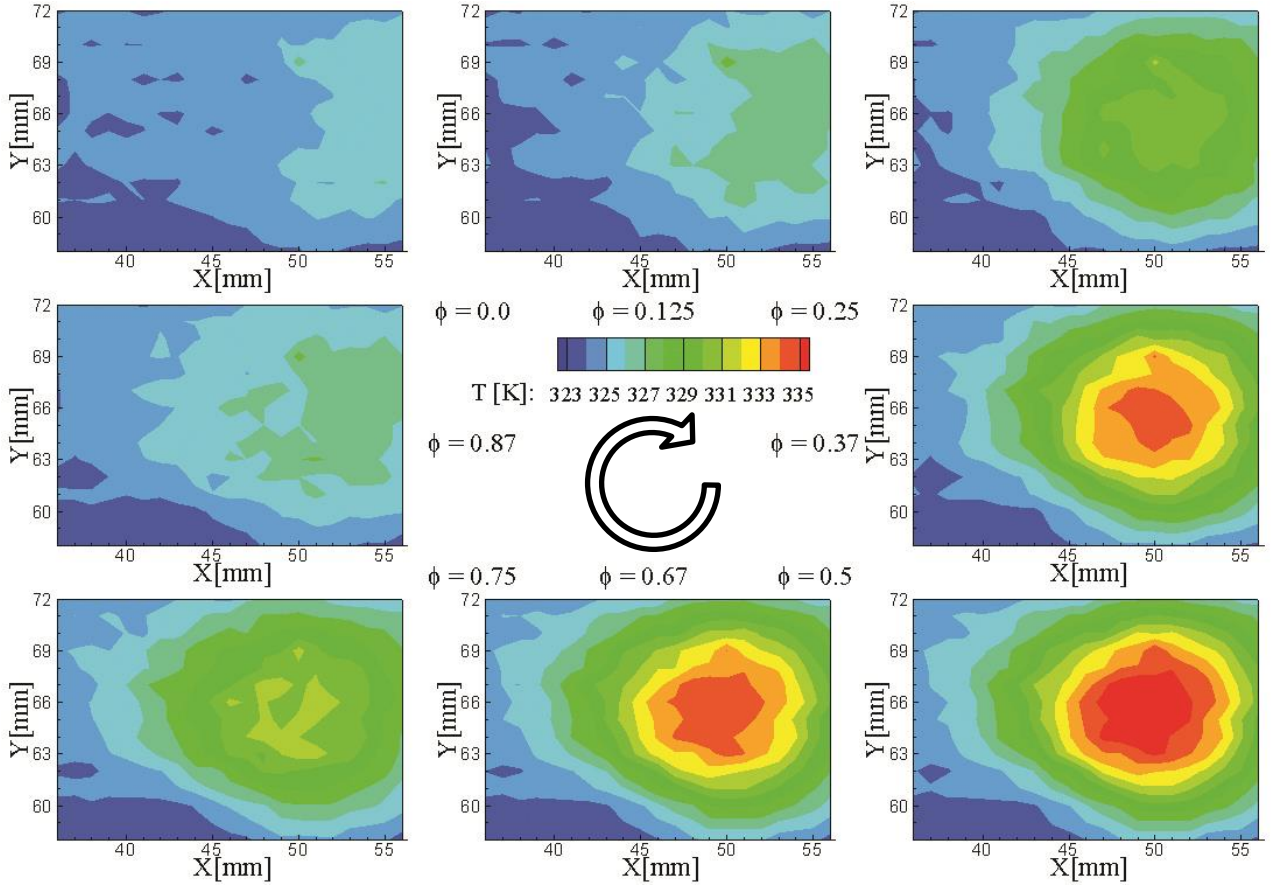
Figure 11: Phase-resolved total temperature field at z = 55 mm, for P_EWG=1.80 bar and n_EWG = 3000 rpm, or 100 Hz

Several technical solutions were studied for the insulation of the hot tubes connecting the EWG core with the injectors, to maximize the amplitude of the entropy waves; an optimal configuration was found by combining a ceramic fiber and a 19 mm elastomeric sheath, which limits the temperature drop on the tube to 40 K for a maximum working temperature exceeding 460 K.

The experimental assessment of the entropy waves generated by the EWG was performed by fast-response total pressure and total temperature probes, specifically developed for the present research program. In particular, micro-thermocouples (~25 μm junction) were manufactured and dynamically calibrated in a shock tube, showing a frequency response exceeding 200 Hz.

The propagation of entropy waves has been discussed considering both free-jet and immersed-jet configurations. In the free-jet condition a sinusoidal temperature oscillation was observed, with amplitude equal to several tens of K at a frequency equal to twice the one of the EWG rotary valve. The amplitude was found to reduce as the EWG frequency increases, probably due to the enhanced mixing between hot and cold air spots as the rotary valve runs at higher speed.

Immersed-jet tests showed a weak aerodynamic effect of the injector and confirmed the sinusoidal character of the entropy wave. However a net reduction of amplitude with respect to free-jet tests was found, with a significant decay as the wave propagates in stream-wise direction. The reduction of amplitude, resulting from the mixing between the jet and the surrounding flow, was minimized by selecting an optimal EWG feeding pressure, identified as the one the guarantees equal momentum between the jet and the surrounding flow. This condition guarantees temperature oscillations exceeding 10 K (~4% of the mean temperature level) at a frequency of 100 Hz.

By virtue of these experimental results, the proposed system outperforms other EWG devices documented in Literature, in terms of amplitude and frequency, as well as for the more realistic character of the entropy waves, and matches the targets of the RECORD project. The proposed EWG is now ready for application in the turbine test-rig for indirect combustion noise experiments.

REFERENCES
Antonini, C., Persico, G., Rowe, A.L. (2008), *Prediction of the dynamic response of complex transmission line systems for unsteady pressure measurements*. Measurement Science and Technology, Vol. 19, pp: 125401

Bake, F., Michel, U., Roehle, I. (2007)*, Investigation of Entropy Noise in Aero-Engine Combustors*, Journal of Engineering for Gas Turbines and Power, Vol. 129, pp. 370-376

Bake, F., Richter, C., Mühlbauer, B., Kings, N., Röhle, I., Thiele, F., and Noll, B. (2009), *The Entropy Wave Generator (EWG): A Reference Case on Entropy Noise*, Journal of Sound and Vibration, Vol. 326, No. 3–5, 2009, pp. 574–598.

Bohn, M. S. (1976), Noise Produced by the Interaction of Acoustic Waves and Entropy Waves with High-Speed Nozzle Flows. Ph.D. thesis, California Institute of Technology, Pasadena, CA.

Churchill, S. W.; Bernstein, M. (1977), *A Correlating Equation for Forced Convection From Gases and Liquids to a Circular Cylinder in Crossflow*, ASME Journal of Heat Transfer, Vol. 99, pp: 300–306.

Cumpsty, N. A. (1979), *Jet Engine Combustion Noise: Pressure, Entropy and Vorticity Perturbations Produced by Unsteady Combustion or Heat Addition*. Journal of Sound and Vibration, 66 (4), pp. 527–544.

Cumpsty, N. A., and Marble, F. E. (1977), *Core Noise From Gas Turbine Exhausts*. Journal of Sound and Vibration, 54 (2), pp. 297–309.

Dowling, A. P. (1996). *Acoustics of unstable flows*. In Theoretical and Applied Mechanics, T. Tatsumi, E. Watanabe, and T. Kambe, eds., Elsevier, Amsterdam, pp. 171–186.

Howe, M. S. (2010), *Indirect Combustion Noise*, Journal of Fluid Mechanics, Vol. 659, pp. 267-288.

Gaetani P., Persico G., Dossena V., Osnaghi C. (2007a), *Investigation of the flow field in a HP turbine stage for two stator-rotor axial gaps - Part I: 3D time average flow field*. ASME Journal of Turbomachinery, Vol. 129, pp. 572 – 579.

Gaetani P., Persico G., Dossena V., Osnaghi C. (2007b), *Investigation of the flow field in a HP turbine stage for two stator-rotor axial gaps - Part II: Unsteady flow field*. ASME Journal of Turbomachinery., Vol. 129, pp. 580 – 590.

Gaetani, P., Persico, G., Osnaghi, C. (2010), *Effects of Axial Gap on the Vane-Rotor Interaction in a Low Aspect Ratio Turbine Stage*. 2010, AIAA Journal of Propulsion and Power, Vol. 26, Issue 2, pp. 325-334.

Leyko, M., Nicoud, F., and Poinsot, T. (2009), *Comparison of direct and indirect combustion noise in a model combustor*, AIAA Journal, vol.47, no.11, pp. 2709-2716.

Leyko, M., Moreau S., Nicoud, F., and Poinsot, T. (2011), *Numerical and analytical modelling of entropy noise in a supersonic nozzle with a shock*, Journal of Sound and Vibration, Vol. 330, pp. 3944-3958.

Lighthill, M.J. (1952), *On sound generated aerodynamically I.* Proceedings of the Royal Society of London, Series A211:564–587.

Lighthill, M.J. (1954), *On sound generated aerodynamically II.* Proceedings of the Royal Society of London, Series A222:1–32.

Marble, F. E., and Candel, S. M. (1977), *Acoustic Disturbances From Gas Non-Uniformities Convected Through a Nozzle*. Journal of Sound and Vibration, 55 (2), pp. 225–243.

Muthukrishnan, M., Strahle, W. C., and Neale, D. H. (1978), *Separation of Hydrodynamic, Entropy, and Combustion Noise in a Gas Turbine Combustor*, AIAA Journal, 16 (4), pp. 320–327.

Persico, G., Gaetani, P., Guardone, A. (2005), Dynamic calibration of fast-response probes in low-pressure shock tubes. *Measurement Science and Technology*, Vol. 16, pp. 1751-1759.

Persico, G., Gaetani, P., Osnaghi, C. (2009), *A parametric study of the blade row interaction in a high pressure turbine stage*. ASME Journal of Turbomachinery, Vol. 131, 031006 (13 pages).

Persico, G., Mora, A., Gaetani, P., Savini, M. (2012), *Unsteady Aerodynamics of a Low Aspect Ratio Turbine Stage: Modeling Issues and Flow Physics*. ASME Journal of Turbomachinery, Vol. 134, 061030 (10 pages)

Rienstra, S.W., and Hirschberg, A. (2015), *An Introduction to Acoustics*. Eindhoven University of Technology

Zukoski, E. E., and Auerbach, J. M. (1976), *Experiments Concerning the Response of Supersonic Nozzles to Fluctuating Inlet Conditions*, ASME Journal of Engineering for Power, Vol. 98, pp. 60–63.